Monthly Notices of the ROYAL ASTRONOMICAL SOCIETY

MNRAS **508,** 2730–2735 (2021) https://doi.org/10.1093/mnras/stab2767
Advance Access publication 2021 September 25

A joint occultation and speckle investigation of the binary star TYC 1947-290-1 and of the asteroid (87) Sylvia

V. Dyachenko,[1]★ A. Richichi,[2] M. Obolentseva,[3] A. Beskakotov,[1] A. Maksimov,[1] A. Mitrofanova[1] and Yu. Balega[1]

[1]*Special Astrophysical Observatory, Nizhnij Arkhyz, Karachai-Cherkessian Republic 369167, Russia*
[2]*INAF – Osservatorio Astrofisico di Arcetri, Largo E. Fermi 5, I-50125 Firenze, Italy*
[3]*Saint Petersburg State University, St Petersburg 198504, Russia*

Accepted 2021 September 21. Received 2021 September 21; in original form 2021 September 13

ABSTRACT

We report on the occultation of the star TYC 1947-290-1 by the asteroid (87) Sylvia. While asteroidal occultations occurring at fixed professional-level locations are relatively rare and are only recently starting to be observed with sufficiently high time resolution and sensitivity, they have the capability to measure sub-milliarcsecond angular diameters. The event described here was especially outstanding because the star was revealed to be a small-separation binary (≈10 mas at discovery), while at the same time the asteroid is not only one of the largest in size but it also has two satellite moons. The observations were carried out at the Russian 6-m telescope in 2019 December, and initially consisted of both a fast photometric series of the occultation itself, as well as of extensive speckle interferometry of the star and asteroid in the time immediately before and after the occultation. Subsequently, we obtained speckle data of TYC 1947-290-1 over a period of 1 yr after the event. We are able to present a detailed study of the binary star including measurements of the angular diameter of the stellar components, their geometry, and relative fluxes over several bandpasses, and to provide an accurate determination of the size of (87) Sylvia. We emphasize that we have been able to obtain the smallest ever directly measured stellar diameter, below the 100 micro-arcsecond level. Our data are also suitable for imaging of the asteroid by speckle holography, a task which we intend to carry out in a separate work.

Key words: instrumentation: high angular resolution – stars: atmospheres – binaries: general.

1 INTRODUCTION

We already highlighted in a previous paper (Dyachenko et al. 2018, hereafter D18) the intrinsic synergy between lunar occultations (LO) and speckle interferometry (SI). The former technique allows us to measure in a model-independent manner sources with any geometry from single stars to binary stars to circumstellar envelopes, with an angular resolution close to the milliarcsecond (mas) level; while the latter is ideally suited to carry out extensive follow-ups in several filters and multiple epochs. We will not discuss here the relative merits and disadvantages, but we note that both techniques require instrumentation capable of millisecond time resolution in a relatively small field of view. At the Russian 6-m telescope, we are in the position to carry out observations with either technique using one common instrument, as already detailed in D18.

In this work, we focus on a variation of the LO method, in which the occulting diffracting edge is provided not by the lunar limb but instead by an asteroid. Asteroidal occultations (AsO) have been employed since several decades, mainly to study the shape of asteroids. They generally consist in observations collected with small movable telescopes *using commercial cameras with relatively slow time resolution*. Extensive examples and literature can be found for example on the IOTA website.[1] More recently, as pioneered by Benbow et al. (2019), such events have raised interest also among observers at large telescopes. In fact, the size of the Fresnel zone projected on Earth is proportional to $D^{1/2}$, where D is the distance from the diffraction screen to the observer. Asteroids being usually at a few au, or few hundred times farther than the Moon, the Fresnel zone is in their case ≈10–30 times more extended. Even allowing for relative speeds of their shadow at Earth a few times faster than in the case of the Moon, the diffraction patterns are significantly more sensitive to small angular diameters than with the LO technique.

We have used the opportunity of an outstanding AsO involving (87) Sylvia, the eighth largest asteroid, and TYC 1947-290-1, a $V = 10.9$ mag star, to study in detail both the occulted star which turned out to be binary, and the asteroid. We describe the observations and the data analysis in Section 2, and discuss the results in Section 3. We summarize our findings and provide an outlook on the potential of the AsO technique with our telescope and instrumentation in Section 4.

2 OBSERVATIONS AND DATA ANALYSIS

The observations were recorded immediately before, during, and after the occultation event on 2019 December 10–12, at the 6-m Large Alt-Azimuthal Telescope (BTA) of the Special Astrophysical

★ E-mail: dyachenko@sao.ru

[1]https://occultations.org/

Table 1. Log of the observations carried out in 2019 December. TYC 1947-290-1 is abbreviated as TYC, (87) Sylvia as SYL. HIP and GAIA are two reference stars, namely HIP 41342 and DR2 707385447274580096, respectively.

Date	Target	Filter	FOV	Frames	DIT	Mode
10-1:35	TYC	550/20	4.″4	2000	50	SI
10-1:40	TYC	700/50	4.″4	2000	20	SI
10-1:43	TYC	800/100	4.″4	2000	20	SI
10-2:17	SYL	700/50	4.″4	4000	50	SI
10-2:29	HIP	700/50	4.″4	4000	50	SI
12-1:06	TYC + SYL	700/50	28.″2	2000	20	P&T
12-1:12	SYL	700/50	6.″7	2000	50	SI
12-1:17	TYC	700/50	6.″7	1000	50	SI
12-1:20	TYC + SYL	700/50	28.″2	1000	50	P&T
12-1:23	TYC + SYL	700/50	6.″7	2000	50	SH
12-1:28	TYC	550/20	6.″7	2000	50	SH
12-1:36	TYC	700/50	5.″6	150000	2.29	AsO
12-1:47	TYC	800/100	6.″7	2000	60	SH
12-1:50	TYC	700/50	4.″4	2000	60	SH
12-1:53	TYC	700/50	6.″7	2000	60	SH
12-1:56	TYC	700/50	6.″7	2000	60	SH
12-1:59	SYL	700/50	4.″4	2000	60	SI
12-2:03	GAIA	700/50	4.″4	2000	60	SI
12-2:07	TYC + SYL	700/50	28.″2	1000	60	P&T
12-2:08	TYC + SYL	700/50	28.″2	1000	60	P&T

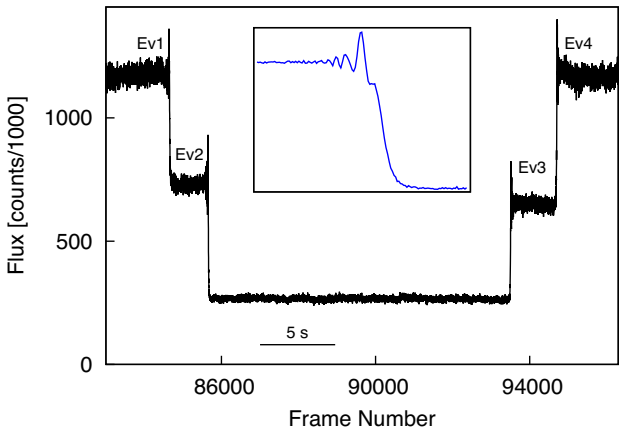

Figure 1. Photometric series of the (87) Sylvia occultation, from the integration of the raw frames in the FITS data cube. The four events are, in chronological order: the disappearances of the primary, of the secondary, and the reappearances of the secondary and, finally, of the primary. Refer also to Fig. 3. The inset shows for comparison a previous unrelated LO light curve of HD 155469, a binary with angular separation and brightness ratio similar to the Ev1-Ev2 pair in this figure. Note how the binary patterns are quite separated in the AsO, while they are overlapping in the LO case. See Section 3.2 for explanation.

Observatory of the Russian Academy of Sciences, in the Caucasus mountains. The predictions for the (87) Sylvia occultation were provided on the http://www.asteroidoccultation.com/ web site.

We used the camera described in D18 to record both a fast 2D imaging series of the occultation event, and various series of speckle data. The log of observations is provided in Table 1, where Date refers to the date in 2019 December followed by the UT time. The column Filter lists the central wavelength and bandpass in nm. FOV is the size of a side of the effective field of view – which was always square. The native pixel size of the detector on the sky is 13 mas, but in some modes rebinning and/or magnification were used. For example, the detector area during the AsO event was 440 × 432 pixels, with a rebinning of 8 × 8, and a magnification of 10, resulting in an effective pixel size of 104 mas, a field of view of 5.″72 × 5.″63 with a FITS frame size of 55 × 54 pixels. DIT is the on-chip integration time, in ms. Modes are SI and SH for speckle interferometry and speckle holography, AsO for the asteroid occultation, and P&T for positioning and timing auxiliary data.

In addition to the TYC 1947-290-1 star and (87) Sylvia asteroid, we also observed HIP 41342 and *Gaia* DR2 707385447274580096 as reference stars.

The AsO raw data are in the form of a FITS cube with frames taken every 2.56 ms. For the purpose of our data reduction, we cropped the frames to 32 × 32 pixels centred on the target. The raw integration of the frames is shown in Fig. 1, and it clearly shows the disappearance of the two components of TYC 1947-290-1, followed by their reapperance. These are marked in temporal sequence as Ev1 through Ev4 in the figure. We will discuss in Section 3.2 how they are related to the primary and secondary component. For the detailed analysis of the diffraction patterns, however, we extracted the stellar signal using a digital mask tailored to the position and shape of the long-exposure image of the star, as described in Richichi et al. (2017) and references therein. Four masks were generated around the time of each event, to minimize possible image motion and drift. In this way, we maximize the signal-to-noise ratio (SNR) by using all stellar signal and the minimum possible contribution from the background.

Only about 0.5 s of data around each of the four events are analysed, as this is sufficient to include all diffraction information. The data are fitted using a least-square model-dependent (LSM) method with a number of free parameters, including the stellar diameter and the speed of the diffraction pattern. The diameter is computed for a uniform disc (UD) model. Our implementation of the method is described in Richichi et al. (1992). Convergence is based on changes in χ^2 values computed from a noise model based on data immediately before and after the occultation.

In addition to the measurements of the star and asteroid listed in Table 1, we also carried out extensive monitoring of TYC 1947-290-1 alone by SI, using various filters and bandpasses, on several different

Table 2. SI results for the TYC 1947-290-1 binary system.

Epoch	Filter	ρ (mas)	θ (°)	Δm (mag)
2019.940286	550/20	32	67.2	0.89
2019.940294	700/50	31	66.8	0.47
2019.940301	800/100	34	65.8	0.79
2020.175108	550/20	36	79.9	–
2020.175115	676/10	32	62.3	–
2020.175121	694/10	38	67.2	–
2020.175128	700/50	37	66.9	0.75
2020.175134	800/100	39	68.2	–
2020.185745	550/20	36	66.8	0.69
2020.185764	676/10	36	64.6	0.86
2020.185776	694/10	37	66.3	0.75
2020.185829	700/50	39	67.9	0.56
2020.185839	800/100	40	68.3	1.34
2020.361042	700/50	43	68.6	0.67
2020.361048	800/100	47	68.6	0.56
2020.674088	550/20	44	71.7	0.81
2020.674084	700/50	40	68.1	0.47
2020.907069	550/20	49	69.3	0.67
2020.907074	700/50	48	71.4	0.41
2020.907082	800/100	48	68.7	0.60

dates from 2020 March to November. These observations are logged in Table 2 along with the corresponding results.

Our SI methodology and data reduction are described in Balega et al. (2002) and Pluzhnik (2005). In summary, we compute the power spectrum averaged over the series and the corresponding autocorrelation function. Modelling of the power spectrum is carried out in a set of rings inside which the speckle profile is assumed to be constant. The parameters of the model for a binary star include the positions and the relative intensities of the components. To eliminate the ambiguity by 180° and obtain a reconstructed image, we use the bispectrum method (Lohmann, Weigelt & Wirnitzer 1983).

Moreover, since the star and the asteroid were so close together to fall inside the same isoplanatic patch, also the technique known as speckle holography (SH) is applicable. In this case, the visibility data of the asteroid can be complemented by phase differences relative to the star. These in turn can be used to reconstruct an actual model-independent image of (87) Sylvia. This task requires significant additional steps in the data selection, analysis, and algorithms. We will deal with it in a separate, dedicated paper.

3 RESULTS

Our results cover a range of aspects on both the target star TYC 1947-290-1 and the asteroid (87) Sylvia. The event was predicted to have a duration of about 28 s and a drop in the stellar flux of about 2.0 mag. This drop is expected to be wavelength dependent in function of the asteroid albedo and of the stellar energy distribution. The asteroid was moving along PA = 315° at the time of occultation.

TYC 1947-290-1 is a $V = 10.9$ mag star with moderately red colours $B - V = 0.4$ mag and $V - K = 1.8$ mag, indicative of a spectral type between F and G. It has high accuracy astrometry from *Gaia*, with the early DR3 reporting 173.3 ± 0.9 pc, thus likely a main-sequence star. There is no mention of its binary nature in the Tycho catalogue and no previous literature entry was available at the time of our observation. While this paper was in preparation, Herald et al. (2020) reported observations of the same event by several small telescopes at different locations in Europe, four of which also revealed TYC 1947-290-1 as binary, albeit without much detail.

(87) Sylvia is the eighth largest asteroid, and has been the subject of several investigations. Marchis et al. (2005) used AO observations to determine the size as an ellipsoid with semi-axes $a = 192$ km, $b = 132$ km, and $c = 116$ km. They also discovered that (87) Sylvia has two moonlets, Romulus and Remus. These are, however, considerably further away and did not occult the target star during our occultation event. Hanuš et al. (2017) used an algorithm based on the combination of AO imaging, light curves, and occultation data to reconstruct the apparent shape of (87) Sylvia, and to show its variations with time. Herald et al. (2020) compared data from different satellite observations to derive a best estimate of the volume equivalent diameter as 267 ± 17 km, in agreement with previous studies (e.g. Berthier et al. 2014).

We discuss first in Section 3.1 the results of the SI investigation of TYC 1947-290-1 as a binary star; we then discuss the occultation findings in Section 3.2.

3.1 The TYC 1947-290-1 binary system

TYC 1947-290-1 was clearly resolved to be binary from the AsO data (see Fig. 1). The binary is within the resolution limits of the 6-m telescope using SI, and we carried out extensive observations over about 1 yr after the occultation event, in a variety of filters. Our results are listed in Table 2. Typical errors are 1 mas in separation and 0.3° in position angle.

Fig. 2 shows that the changes in separation ρ and position angle θ can be initially tentatively interpreted as a bound orbit with a very low inclination angle. The fitted period and total mass would be of order ≈30.7 yr and ≈3 $M_\odot$, consistent with the expected masses for main-sequence stars of F-G spectral types. We stress that this result is very preliminary and the values might well change with additional follow-up measurements. We also note that the nearest star of comparable brightness lies 5 arcmin away, hinting at a very small likelihood of TYC 1947-290-1 being a visual binary.

We have inspected the magnitude differences between the two components, with one entry from Table 2 having $\Delta m = 1.34$ removed as an obvious outlier. In spite of a large scatter due to the difficulty of obtaining precise SI measurements on a source close to the diffraction limit of the telescope, we find that there is no obvious trend with filter nor with epoch. We conclude that Δm is on average 0.66 ± 0.11 mag and that the two components should be of similar spectral type.

3.2 The asteroidal occultation (AsO)

To help in the interpretation, we have sketched the geometry of the event in Fig. 3, which is, however, only indicative.

For this, we have generated the predicted shape of (87) Sylvia from the Database of Asteroid Models from Inversion Techniques (DAMIT; Ďurech, Sidorin & Kaasalainen 2018). At the time of our occultation, the projected transverse size was 308 km, with our site placed about 52 km off the ground track centre (courtesy of H. Pavlov). At the predicted distance of 2.918 au, the transverse size projected to 145.5 mas on the sky. In Fig. 3, we have assumed that the star coordinates coincide with the primary. Knowing its binary nature, this is not strictly correct but the scheme remains valid.

As the asteroid moved along PA = 315° over the TYC 1947-290-1 system, two disappearance and two reappearance events took place as shown in Fig. 1. The two components appear to have comparable fluxes at 700 nm, and ordering them in the occultation sequence is open to some uncertainty. Fig. 1 rather convincingly indicates that F(Ev1) > F(Ev2) and F(Ev3) < F(Ev4), pointing at the primary disappearing first and reappearing last. This is supported also by the

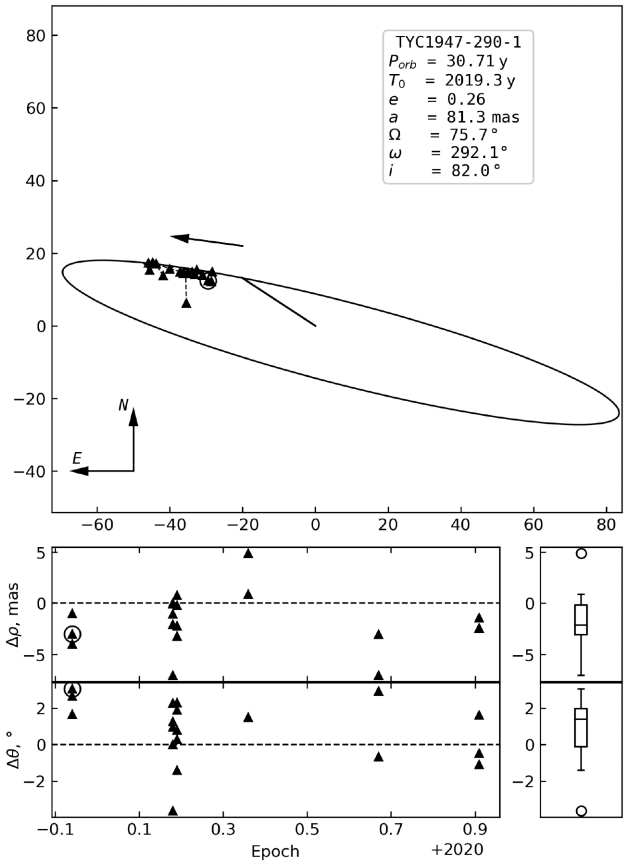

Figure 2. One of the family of orbital solutions for TYC-1947-290-1 pair. Due to the small coverage of the orbital arc and significant relative measurement errors, this solution has a preliminary status. The lower panels show the residuals of angular separation and position angle (left), and their distribution (right).

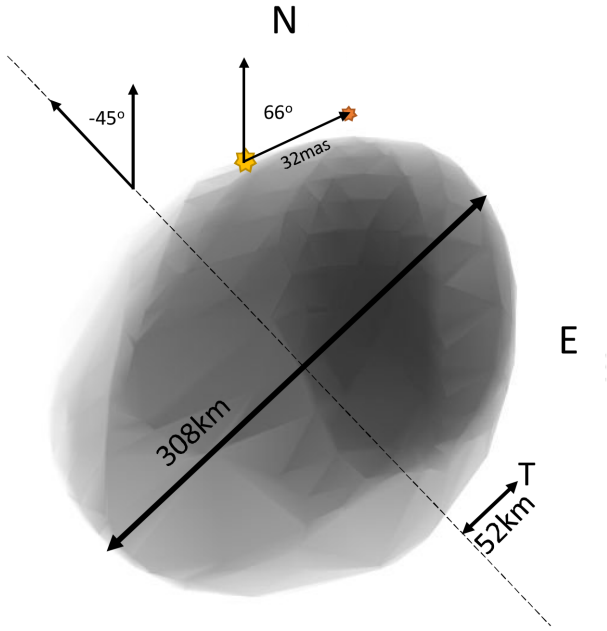

Figure 3. Schematic representation of the occultation of the binary star TYC 1947-290-1 by asteroid (87) Sylvia, resulting in the four events marked in Fig. 1. The asteroid shape is based on the DAMIT model, and the brightness distribution is rendered in negative. The dashed line is the asteroid ground track, with T marking the offset of the 6-m telescope from the track centre. The view is from the star to Earth. See the text for further details.

Table 3. Asteroidal occultation timing results.

Event (1)	ΔTime (ms) (2)	Ang. rate (mas s^{-1}) (3)	Proj. sep. (mas) (4)
Ev1	0	3.7732 ± 0.0028	0
Ev2	2571.7 ± 1.4	3.9894 ± 0.0037	10.26 ± 0.01
Ev3	22608.5 ± 1.3	4.2623 ± 0.0037	96.36 ± 0.08
Ev4	25678.8 ± 1.6	4.2924 ± 0.0038	110.22 ± 0.10

Table 4. Fit results for the four events of Fig. 4. We explain in the text that the diameter value in parentheses is likely affected by limb irregularities.

Event (1)	Star (2)	ϕ (mas) (3)	V_L (m/ms) (4)	CA (°) (5)	$-\Delta\chi^2_n$ (6)
Ev1	P	(0.089 ± 0.002)	7.976 ± 0.016	31.4	26%
Ev2	S	0.035 ± 0.002	8.917 ± 0.007	17.4	1%
Ev3	S	0.028 ± 0.003	−9.149 ± 0.007	168.2	0%
Ev4	P	0.052 ± 0.001	−9.020 ± 0.008	164.8	7%

scheme outlined in Fig. 3 and by the occultation timings listed in column 2 of Table 3, and is therefore our preferred interpretation.

We recognize that Fig. 1 also shows that F(Ev2) ≠ F(Ev3) and F(Ev1) ≠ F(Ev4). We attribute this apparent discrepancy to signal fluctuations. By computing average signal levels over long portions excluding the parts with occultation fringes, we confirm that our hypothesis is valid within errorbars.

To illustrate the great advantage in angular resolution afforded by the expanded Fresnel scale for AsOs compared to LOs, we have included in Fig. 1 an inset with the occultation data of HD 155469 (from Richichi et al. 2014; Fig. 1). This binary star had a projected separation well comparable with the Ev3-Ev4 pair of Fig. 1. The pair observed by LO has largely overlapping Fresnel patterns, while in the AsO case they are completely separated.

We start by discussing the angular separations between the four events of Fig. 1, which are derived from the relative time differences and the angular rates as listed in Table 3. Note that the fringe rate is different from each event, as expected, so that we used an interpolation between the best-fitting values derived for each event, as described below and listed in column 4 of Table 4.

It can be seen that the separation between primary and secondary is different at disappearance and reappearance, namely 10.3 and 13.9 mas, respectively, in line with the fact that the contact angles are also different (cf. Table 4). The average is ≈12.1 mas, which matches very well the speckle values after projection. The length of the cords across (87) Sylvia is 110.2 mas (or 233.3 km) for the primary, and 86.1 mas (or 182.3 km) for the secondary. This is well consistent with the scheme of Fig. 3.

Concerning the angular diameters of the components of TYC 1947-290-1, we extracted the light curves for each individual event using a mask-based method as explained in Section 2. This led to the four data sets shown in Fig. 4, which for convenience have been rescaled to arbitrary zero-points and intensity units. Already by eye it can be appreciated that the light curves for Ev2 and Ev3, those for the secondary, display more diffraction fringes than those for the primary, in agreement with a smaller angular diameter for the former.

The four light curves were fitted with the LSM method described in Section 2.

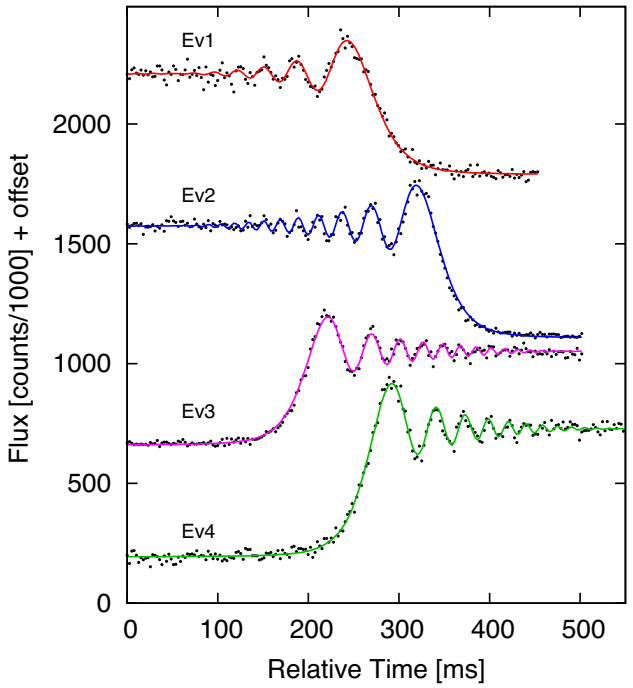

Figure 4. Occultation data (dots) and best fits by a stellar disc (lines) for the four occultation events of TYC 1947-290-1 isolated from Fig. 1. Both the intensity and the zero times of the events are shifted by arbitrary offsets for clarity of presentation. Ev1 and Ev4 are the disappearance and reappearance of the primary, Ev2 and Ev3 of the secondary.

The results of these fits are listed in Table 4, where the first two columns refer to the event in Fig. 1 and the primary or secondary nature of the component. Further listed are the angular diameter ϕ and linear velocity of the fringe pattern V_L determined as free parameters in the fit, along with their formal errors. CA is the contact angle derived from the difference between the fitted V_L and the predicted speed of 9.3465 m/ms, and is an indication of the local slope of the asteroid limb. CA would be 0° for a limb perpendicular to the direction of motion. Finally, the table lists the improvement in normalized χ^2 of the fit, going from a point-like to a resolved source model.

The χ^2_n is computed from a noise model which for each event includes read-out noise and photon shot noise derived from the occulted and unocculted portions of the light curve. In explicit terms, a fit to the light curve of Ev1 using a point-like source yields $\chi^2_n = 1.325$, while the best-fitting model with an angular diameter of 0.089 mas yields $\chi^2_n = 0.986$.

The CA values show that the curvature of the asteroid limb is significant even on the small angular scales which separate the two components. This is not unexpected given that the asteroid transverse angular size at the predicted distance of 2.918 au was 145.5 mas, or just ≈4 times the angular separation of the binary.

Taking into account the relative improvement in χ^2_n (Table 4, last column), we reach different conclusions for the primary and the secondary of TYC 1947-290-1. Starting with the secondary (Ev2 and Ev3), we conclude that it is unresolved, with an averaged upper limit of ≈0.031 mas in angular diameter.

As for the primary, the two values (Ev1 and Ev4) are widely different, well outside the formal errorbars. In our experience, and indeed from diffraction theory, it is possible to mimic fringes with lesser contrast than real, but not with higher contrast. In other words, it is possible that bias effects might make a star appear larger than reality. As we already take into account all instrumental effects in our analysis, the most likely explanation left would be fringe smoothing due to limb irregularities. In the field of LOs, such a scenario was discussed already by Murdin (1971), who found that in order to affect the diffraction curve, the lunar limb should have highly aligned structure along the line of sight. This is difficult to realize for a large body like the Moon, but is not unrealistic in the case of a smaller body like (87) Sylvia.

We also considered the possibility that the straight-edge may not be a good approximation in our case, and whether the formalism for a circular diffracting edge developed by Roques, Moncuquet & Sicardy (1987) could be more appropriate. However, following the simulations by Jennings & McGruder (1999), we find that the straight-edge approximation results in a maximum intensity error of <4 per cent. In fact, when averaged over the light curve and when instrumental effects are added, the difference in fringe intensity becomes negligible and cannot account for the difference in Ev1 and Ev4 diameters. We thus take the approach that the larger diameter measured at Ev1 is possibly affected by limb structure, and we adopt the value measured at Ev4.

For comparison, we note that at the *Gaia* EDR3 distance of 173.3 pc our upper limit for the TYC 1947-290-1 secondary corresponds to ≈0.6 $R_\odot$, while for the primary the measured value is ≈1 $R_\odot$. This is roughly consistent with the *Gaia* EDR3 fitting template temperature of 5500 K (compare with Boyajian et al. 2013, fig. 11). Since we deduced similar spectral types of the two components in Section 3.1, their magnitude difference would lead to an expected 1:1.35 diameter ratio, roughly comparable to the ≥1.6 ratio that we measure. On the other hand, our preliminary orbital fit gave a total mass of ≈3 $M_\odot$, consistent with a main-sequence F-G star as indicated by the Tycho colours but pointing at a diameter larger than solar. This apparent discrepancy is probably explained by the fact that the *Gaia* EDR3 model assumes a single star. In fact, already the DR2 parallax was 2.5σ larger than in EDR3, pointing at difficulties in the *Gaia* model. Further, as already stated, our orbital fit should be considered as very preliminary and we do not exclude significant revisions of the total mass.

In conclusion, our measured diameter of 0.052 mas for the primary and upper limit of 0.031 mas for the secondary are generally consistent with the expected values, within the limits of our current knowledge for this system. Rather than using the formal errors of Table 4, from the discussion above we estimate that a 10 per cent relative error is more appropriate.

4 CONCLUSIONS AND FUTURE OUTLOOK

We analysed an occultation of the star TYC 1947-290-1 by the asteroid (87), resulting in the detection of the star as binary and yielding angular diameters of 0.052 and ≤0.031 mas for the primary and secondary, respectively. At the *Gaia* distance of 173 pc, these values are well consistent with two solar type stars.

We also carried out speckle observations immediately before and after the occultation event, as well as monitoring of the system for about 1 yr. We derive separations and position angles for the system at a number of epochs, and are able to provide a first preliminary orbit with a high inclination, a low eccentricity, period ≈30 y, total mass ≈3 $M_\odot$, and ≈0.081 mas (14 au) semimajor axis. These values are subject to possibly significant revision as more orbital points will be measured.

All measurements were carried out at the Russian 6-m telescope of the SAO RAS, using the same speckle interferometer instrument,

demonstrating once more the synergy between occultations and speckle (see D18).

With the advances in long-baseline interferometry (LBI), the role of single telescopes in obtaining high angular resolution data has been sidelined: indeed, LO allows a resolution of about 1 mas, comparable with the present capabilities of LBI at optical and infrared ranges. Recently, the use of star occultations by asteroids (Benbow et al. 2019) has shown that resolutions at the 0.1 mas level are possible for observations with single optical telescopes. In this work, we have reached for the first time a resolution of ≈50 μas in the optical range.

The probability of AsOs from a given site is small, due to the narrow size of the ground track and inherent uncertainties in the orbit. For this reason, AsOs have been traditionally carried out with small movable telescopes with relatively low performance in terms of time resolution and SNR. Thus, they were usually limited to determining the asteroidal properties. A large telescope capable of ms time resolution, however, changes completely the context and enables accurate measurements of the stellar properties as well. At a site like the Russian 6-m telescope, we have already observed a few such events in the course of 1 yr (results to be presented elsewhere), and it is hoped that more similar facilities can be used soon for such observations, allowing us resolutions tens of times smaller than by LO or LBI, and 1000 times smaller than the diffraction limit of single large telescopes.

ACKNOWLEDGEMENTS

This study was funded by RFBR, project number 20-32-70120. The work was performed as part of the government contract of the SAO RAS, approved by the Ministry of Science and Higher Education of the Russian Federation. This research has made use of the SIMBAD database, operated at CDS, Strasbourg, France. Predictions for the event were obtained from the site http://www.asteroidoccultation.com/, and we gratefully acknowledge the help of H. Pavlov for the detailed asteroid ground track.

DATA AVAILABILITY

The data underlying this article will be shared on reasonable request to the corresponding author.

REFERENCES

Balega I. I., Balega Y. Y., Hofmann K.-H., Maksimov A. F., Pluzhnik E. A., Schertl D., Shkhagosheva Z. U., Weigelt G., 2002, A&A, 385, 87
Benbow W. et al., 2019, Nat. Astron., 3, 511
Berthier J., Vachier F., Marchis F., Ďurech J., Carry B., 2014, Icarus, 239, 118
Boyajian T. S. et al., 2013, ApJ, 771, 40
Dyachenko V., Richichi A., Balega Y., Beskakotov A., Maksimov A., Mitrofanova A., Rastegaev D., 2018, MNRAS, 478, 5683 (D18)
Ďurech J., Sidorin V., Kaasalainen M., 2010, A&A, 513, A46
Hanuš J. et al., 2017, A&A, 601, A114
Herald D. et al., 2020, MNRAS, 499, 4570
Jennings J. K., McGruder C. H., 1999, AJ, 118, 3061
Lohmann A. W., Weigelt G., Wirnitzer B., 1983, Appl. Opt., 22, 4028
Marchis F., Descamps P., Hestroffer D., Berthier J., 2005, Nature, 436, 822
Murdin P., 1971, ApJ, 169, 615
Pluzhnik E. A., 2005, A&A, 431, 587
Richichi A., di Giacomo A., Lisi F., Calamai G., 1992, A&A, 265, 535
Richichi A., Fors O., Cusano F., Ivanov V. D., 2014, AJ, 147, 57
Richichi A. et al., 2017, MNRAS, 464, 231
Roques F., Moncuquet M., Sicardy B., 1987, AJ, 93, 1549

This paper has been typeset from a TEX/LATEX file prepared by the author.